Digital Communications and Networks 2 (2016) 77–83

HOSTED BY

ELSEVIER

Contents lists available at ScienceDirect

Digital Communications and Networks

journal homepage: www.elsevier.com/locate/dcan

Wavelet networks for reducing the envelope fluctuations in WirelessMan–OFDM systems

Radouane Iqdour [a,*], Younes Jabrane [b]

[a] Regional Center for Education Careers and Training, Marrakesh, Morocco
[b] OSCARS Laboratory National School of Applied Sciences, Cadi Ayyad University, Marrakesh, Morocco

ARTICLE INFO

Article history:
Received 11 December 2015
Received in revised form
9 February 2016
Accepted 25 February 2016
Available online 5 March 2016

Keywords:
WiMAX/OFDM
PAPR reduction
Wavelet Network
Cubic metric
ACE-AGP

ABSTRACT

The IEEE 802.16d standard specified Orthogonal Frequency Division Multiplexing (OFDM) modulation for the Worldwide Interoperability for Microwave Access (WiMAX) physical layer. However, the main weakness of OFDM is the high Peak-to-Average Power Ratio (PAPR). In this paper, we present two new approaches based on Wavelet Networks (WNs) for reducing the PAPR in the fixed WiMAX system. The training data is obtained from the ACE-AGP algorithm. The results of the simulations show the effectiveness of the proposed schemes even for high order modulation such as 64-QAM. Furthermore, the proposals allow reduction in the complexity and convergence time in comparison with other methods.

Contents

1. Introduction

The WiMAX technology has recently gained in popularity due to its scalability in both radio access and network architecture as well as high-throughput broadband connection over long

* Corresponding author.
E-mail addresses: radouane.iqdour@taalim.ma (R. Iqdour), y.jabrane@uca.ac.ma (Y. Jabrane).
Peer review under responsibility of Changing University of Posts and Telecommunications.

http://dx.doi.org/10.1016/j.dcan.2016.02.002

distances. For better service quality in terms of bandwidth and available frequency spectrum, the WirelessMan–OFDM based on IEEE 802.16d is associated with high speed modulation such as OFDM [1,2].

The OFDM is a multicarrier modulation technique that has many advantages such as high bandwidth efficiency, robustness to the selective fading problem, use of a small guard interval, and the ability to combat the inter-symbol interference problem [3]. However, it suffers from a serious weakness, the approximately Gaussian-distributed output samples cause large envelope fluctuations. Therefore, WiMAX hardware equipment is exposed to non-linearity caused by the problem of the high PAPR in OFDM multi-carrier signals.

In the last decade, several techniques and algorithms for PAPR reduction have stimulated great interest [4]. These techniques include amplitude clipping and filtering, coding [1], Tone Reservation (TR) and Tone Injection (TI), Active Constellation Extension (ACE) [5], Partial Transmit Sequence (PTS), Selected Mapping (SLM) [6,7], and the Sequential Quadratic Programming (SQP) algorithm [8]. These differ in terms of the requirements and restrictions they impose on the system. Other methods based on artificial intelligence techniques, notably fuzzy neural networks, have also been proposed in [9,10]. These methods give good performance in terms of PAPR reduction with low complexity, although high density modulations such as 64-QAM were not taken into account by the authors. In this paper, we extend the method proposed in [10] by considering the PAPR problem in WirelessMan–OFDM systems and by using Wavelet Networks (WNs) to construct a scheme able to reduce the PAPR. On the other hand, we tested the validity of our proposal for high density modulations such as 64-QAM.

The WNs are a new class of networks that take advantage of high resolution wavelets, learning and the feed forward nature of neural networks [11]. A motivation for using Wavelet Networks is its great success in a wide range of applications [12]. The training data of the WNs is obtained from the ACE-AGP method since it provides considerable envelope reductions without the need for side information, so that the data rate is not compromised. Its only weakness is its slow convergence that requires a long processing time to obtain the desired signal.

This paper is organized as follows: In Section 2, we present the PAPR problem in the OFDM system. Section 3 introduces the principle of Wavelet Networks. The proposed models are then detailed and analyzed in Section 4. The performance of the proposed models for WirelessMan–OFDM PHY-layer is presented and discussed in Section 5. Finally, the conclusions are given in Section 6.

2. System model

Consider a WirelessMan–OFDM system, where the data is represented in the frequency domain. The time-domain complex baseband transmitted signal x^{ℓ} for the $\ell-$th symbol can be written as

$$x^{\ell} = \{x^{\ell}[0]\ldots x^{\ell}[N-1]\}^{\mathrm{T}} = \left(\frac{1}{\sqrt{N}}\sum_{k=1}^{N-1} S_k^{\ell}\right) e^{\frac{j2\pi kn}{N}} \tag{1}$$

where N is the number of subcarriers and S_k^{ℓ} is the frequency domain complex base-band symbol modulated on the $k-$th subcarrier at OFDM symbol ℓ.

In the case of IEEE 802.16d, QPSK, 16-QAM and 64-QAM constellations are used.

2.1. Cubic metric

PAPR is the most common measure of the envelope fluctuations of an OFDM signal. However, this metric does not appropriately take into account the distortion effect due to the nonlinear response of the High Power Amplifier (HPA). Hence, the Cubic Metric (CM) has been adopted by the 3GPP member [13] as an accurate performance measure replacing PAPR. This metric, which uses the third moment of the transmit signal, can be judged as a better representation of the influence of the HPA. It is defined by the following expression:

$$CM = \frac{RCM_{(\mathrm{dB})} - RCM_{\mathrm{Ref}(\mathrm{dB})}}{K}(\mathrm{dB}) \tag{2}$$

where RCM is the Raw Cubic Metric defined for a signal x as

$$RCM = 20\log_{10}\left(RMS\left(\frac{|x|}{RMS(x)}\right)^3\right) \tag{3}$$

RCM_{Ref} is 1.52 dB, and K is 1.56 for multi-carrier systems.

2.2. ACE-AGP method

The Active Constellation Extension (ACE) technique [13] method intelligently shifts outer constellation points within an allowable region which does not affect the demodulation slicer. Fig. 3 (red points) shows the corresponding extension of each point for QPSK and 16 QAM modulations. Several versions of this algorithm are provided [13]. In this paper, the Approximate Gradient-Project (AGP) is used since it generates OFDM signals with very low envelope fluctuations, less iterations and without side information. To minimize the peak value by the ACE-AGP method, the constellations of the signal are moved such that the PAPR of the time domain is reduced and the minimum distance between constellation points does not decrease. This algorithm is formulated by considering the clipped portion of the signal $\boldsymbol{c}_{\mathrm{clip}}$, which is expressed as

$$\bar{x}[n] = x[n] + \boldsymbol{c}_{\mathrm{clip}}[n] \tag{4}$$

where $\bar{x}[n]$ is the signal with reduced maximal amplitude modulus, and

$$\boldsymbol{c}_{\mathrm{clip}}[n] = \begin{cases} 0, & |x[n]| \le A \\ \left(A - |x[n]|\right)e^{j\theta[n]}, & |x[n]| > A \end{cases} \tag{5}$$

The iterative signal update can be written as:

$$x^{i+1} = x^{i} + \mu c \tag{6}$$

where i is the number of the iteration, μ is the gradient step size and c is the extended time sequence. This process ends with an acceptable PAPR or when a maximum iteration count is reached.

3. Wavelet network

WNs combine classic sigmoid Neural Networks (NNs) and the Wavelet Analysis (WA). It usually has the form of a three layer network that uses a wavelet as the activation function. The lower layer represents the input layer, the middle layer is the hidden layer, and the upper layer is the output layer. In the input layer, the input variables are introduced to the WN. The hidden layer consists of the Hidden Units (HUs). The HUs are often referred to as wavelons similar to neurons in the NNs. In the hidden layer, the input variables are transformed to dilated and translated versions

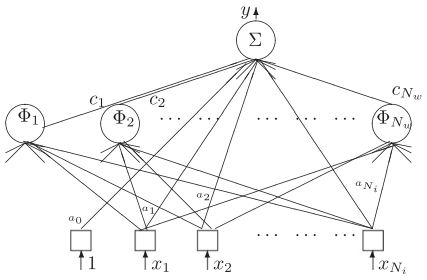

Fig. 1. Feed-forward Wavelet Network.

of the mother wavelet. Finally, in the output layer the approximation of the target values is estimated [11].

In this paper, we use a simple feed-forward WN structure with one hidden layer embedding four HUs and a linear connection between the wavelons and the output. The structure of a general single hidden-layer feed-forward WN is given in Fig. 1. The network output is as follows:

$$y = \sum_{j=1}^{N_w} w_j \Phi_j(x) + \sum_{k=0}^{N_i} a_k x_k \quad \text{with } x_0 = 1 \tag{7}$$

In the expression above $\Phi_j(x)$ is a multidimensional wavelet which is constructed by the product of N_i scalar wavelets, $x = (x_1, x_2, \ldots, x_{N_i})$ is the input vector, N_w is the number of HUs, and w stands for a network weight. The multidimensional wavelets are computed as follows:

$$\Phi_j(x) = \prod_{k=1}^{N_i} \phi(z_{jk}), \tag{8}$$

where ϕ is the mother wavelet and

$$z_{jk} = \frac{x_k - m_{jk}}{d_{jk}} \tag{9}$$

where m_j and d_j are the translation and dilation vectors $(d_j > 0)$ respectively. In the present paper, we choose the first derivative of a Gaussian function, as the mother wavelet,

$$\phi(x) = -xe^{\frac{1}{2}x^2} \tag{10}$$

After the initialization phase, the WN is further trained using the Levenberg–Marquardt algorithm [14] in order to find signals with low envelope fluctuations. Various methods have been proposed for an optimized initialization of the wavelet parameters. Therefore, we use the following initialization (based on the input domains defined by the examples of the training sample) for the translation and dilation parameters [15]:

$$m_j = 0.5(MX_j + MI_j) \tag{11}$$

$$d_j = 0.2(MX_j - MI_j) \tag{12}$$

where MX_j and MI_j are defined as the maximum and minimum of input x_j respectively.

The initialization of the direct connections a_k and the weights w_j are less important and they are initialized with small random values between 0 and 1.

4. Proposed models

4.1. Time WN model

In this section, a Time WN (TWN) model is developed to learn which time-domain signals display low envelope fluctuations. This model is trained using the signals with low envelope fluctuations achieved by the ACE-AGP algorithm. Given that the WN system only works with integer data, we first decompose the time domain of the original signal into real and imaginary parts to reduce the complexity. The training process is detailed as follows [9]:

1. Use the original time-domain data x as an input to the ACE-AGP algorithm to obtain x^{AGP}, i.e., a signal with reduced envelope fluctuations.
2. Split x and x^{AGP} into two sets, namely, the training set x^{tr}, $x^{\mathrm{AGP,tr}}$ and the test set x^{ts}, $x^{\mathrm{AGP,ts}}$.
3. Decompose the original data into real and imaginary parts x^{tr}, $(x_{\mathrm{Re}}^{\mathrm{tr}}, x_{\mathrm{Im}}^{\mathrm{tr}})$, and ACE-AGP output, $x^{\mathrm{AGP,tr}}$ $(x_{\mathrm{Re}}^{\mathrm{AGP,tr}}, x_{\mathrm{Re}}^{\mathrm{AGP,tr}})$.
4. Obtain $x_{\mathrm{Re}}^{\mathrm{T}}$ and $x_{\mathrm{Im}}^{\mathrm{T}}$ by training the two models $Mod_{\mathrm{Re}}^{\mathrm{T}}$ and $Mod_{\mathrm{Im}}^{\mathrm{T}}$, with the pairs $[x_{\mathrm{Re}}^{\mathrm{tr}}, x_{\mathrm{Re}}^{\mathrm{AGP,tr}}]$ and $[x_{\mathrm{Im}}^{\mathrm{tr}}, x_{\mathrm{Im}}^{\mathrm{AGP,tr}}]$ respectively.
5. Test with the values of x^{ts} to validate the models $Mod_{\mathrm{Re}}^{\mathrm{T}}$ and $Mod_{\mathrm{Im}}^{\mathrm{T}}$.

4.2. Time–Frequency WN model

To overcome the problem of the TWN model, we use the Time Frequency WN (TFWN) model. The principle of this scheme is to employ the frequency-domain of the output signal of the first scheme (Fig. 2) as input and the frequency-domain ACE-AGP signals as desired output. The training procedure is as follows [9]:

1. Apply DFT on $x_{\mathrm{Re}}^{\mathrm{T}}$ and $x_{\mathrm{Im}}^{\mathrm{T}}$ to obtain the frequency-domain signal X^{T}.
2. Split the data into training samples $X^{\mathrm{T,tr}}$ and test samples $X^{\mathrm{T,ts}}$.
3. Separate the training samples $X^{\mathrm{T,tr}}$ in the four constellation regions in order to train eight WNs. We will divide the signal into two sets: first set concerning real parts and the second set concerning the imaginary parts, as seen in Fig. 2.
4. Train the first set of WNs by $\Re e(X^{\mathrm{T,tr}})$ to generate $Mod_{\mathrm{Re,1q}}^{\mathrm{TF}}$, $Mod_{\mathrm{Re,2q}}^{\mathrm{TF}}$, $Mod_{\mathrm{Re,3q}}^{\mathrm{TF}}$ and $Mod_{\mathrm{Re,4q}}^{\mathrm{TF}}$ for each quadrant.
5. Train the second set of WNs by $\mathrm{Im}(X^{\mathrm{T,tr}})$ to generate $Mod_{\mathrm{Im,1q}}^{\mathrm{TF}}$, $Mod_{\mathrm{Im,2q}}^{\mathrm{TF}}$, $Mod_{\mathrm{Im,3q}}^{\mathrm{TF}}$ and $Mod_{\mathrm{Im,4q}}^{\mathrm{TF}}$ for each quadrant.
6. Test with the values of $X^{\mathrm{T,ts}}$ to validate the models.

4.3. Complexity analysis

In order to compare the performance of the proposed models, we perform a complexity comparison with the most popular approaches and algorithms such as the Partial Transmit Sequence (PTS), Selective Mapping (SLM) algorithms and two recent modified (less complex) versions for the PTS [5] and the SLM [6], where U and M are the numbers of blocks and sequences, respectively. The complexity of the ACE-AGP algorithm in terms of complex multiplications and additions is $N_{iter}(2N + N/2\log_2(N))$ and $N_{iter}(4N + N\log_2(N))$, respectively, where N_{iter} is the number of iterations, while for the PTS algorithm the complexity in terms of complex multiplications and additions is $2NM + (U(N/2\log_2(N)))$ and $MN(2(U-1)+1) + (U(N\log_2(N)))$, respectively.

The number of complex multiplications and complex additions required in the original SLM scheme is $(N/2)\log_2(N)U + NU^2$ and $N\log_2(N)U$ respectively. In the modified SLM scheme, additional $N(U^2 - U)$ complex additions are needed.

It is important to note that the WNs' proposed models, once they have been identified, basically perform integer operations (multiplications and additions) to obtain the desired output. Generally, the number of operations to compute the output for a WN system is $N_{tot} = 3N_w(N_i + 2) + N_i + 1$ (in this paper: N_w=4, N_i=1). Thus, the complexity of the TWN and the TFWN proposals in terms of number of integer multiplications and additions per OFDM symbol is, respectively, $2N_{tot}N$ and $8N_{tot}N$. The main results of this comparison are summarized in Tab. 1.

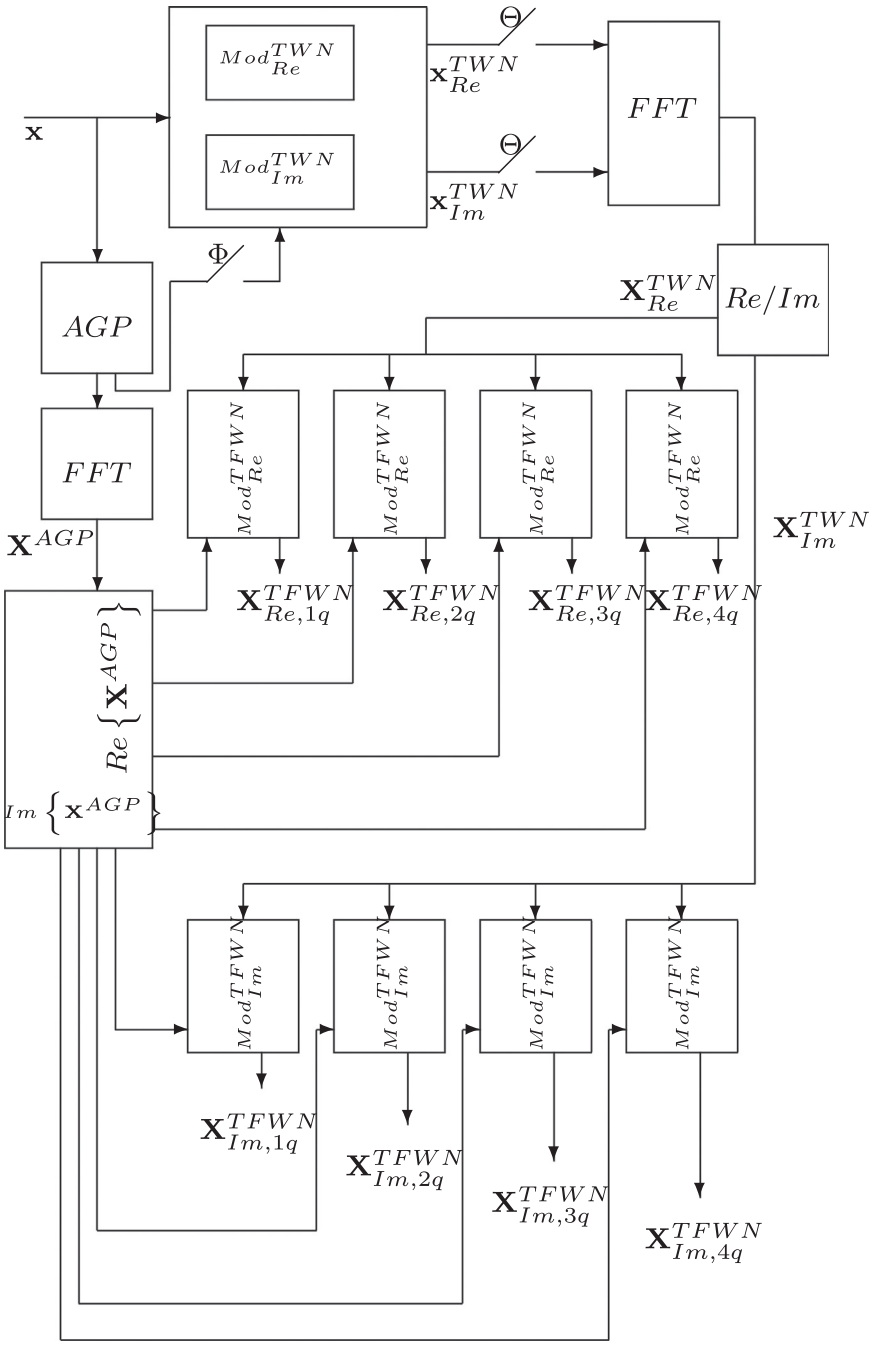

Fig. 2. For TWN training: Switch *Φ on* and *Θ off*. For TFWN training: Switch *Φ off* and *Θ on*.

Tab.1
Complexity summary and comparison for different methods (N=256).

	Original SLM U=16	Modified SLM U=4	Original PTS U=8, M=64	Modified PTS U=8,M=16	ACE-AGP N_{iter} =50	TWN model	TFWN model
(I)FFT	16	4	64	16	100	-	2
Complex Mult	81,920	8192	40,960	16,384	76,800	-	2048
Complex Adds	32,768	35,840	262,144	77,824	153,600	-	4096
Integer operations (Adds, Mult)	–	–	–	–	–	38,912	77,824

According to Tab.1, the proposed models are much less complex than the other schemes, especially, the TWN model does not need any (I)FFT operations, whereas the TFWN model requires only two. In addition, the operations that our proposals need are even simpler than the other schemes (only complex operations are needed for the TFWN scheme when applying the FFT).

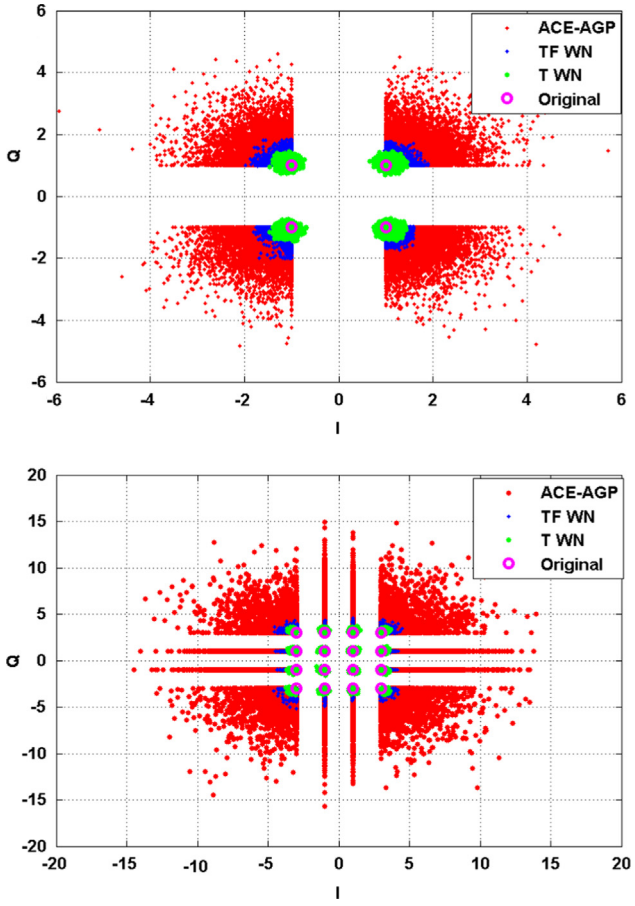

Fig. 3. Constellation after ACE-AGP and the proposed time-domain WN and Time–frequency-domain WN for QPSK (above) and 16-QAM.

4.4. Training phase

The training data employs an OFDM signal with $N=256$ subcarriers using QPSK and 16 QAM modulation. For the ACE-AGP, the maximum number of iterations was fixed to be 2000 (i.e., a large number of iterations to guarantee its best performance). Once the training database is defined, we proceed to the second stage which consists of estimating the models' parameters.

In Fig. 3, we compare the obtained constellation, for QPSK and 16-QAM modulation, from the ACE-AGP and the WNs' proposed models obtained in the training stage. From these figures, we show that there are some symbols placed into the not-allowable region for the TWN model, which can cause performance degradation. Hence, a second WN scheme working on the frequency domain is proposed. In the case of the frequency domain, we easily observe from Fig. 3 that the constellation obtained by the TFWN model has the same behavior as that provided by the ACE-AGP algorithm. Thus, the developed models seem to be adequate for reducing PAPR in WiMAX/OFDM systems. In addition, the two WN proposed models concentrate more energy comparing to ACE-AGP algorithm: the average constellation energy for the original signal is 1 for QPSK (and 5 for 16-QAM), for ACE-AGP it is 1.29 (5.73), for the TWN it is 1.12 (5.4) whereas for TFWN it is 1.2 (5.42).

5. Simulation results

In this section, the proposed PAPR reduction models for a system based on IEEE 802.16d are simulated. The simulation results are obtained for a WirelessMan–OFDM PHY-layer based on IEEE 802.16d which stipulates the use of a total of 256 subcarriers, such as 192 data carriers (QPSK, 16 QAM or 64 QAM signal mapping), 8 pilots, as well as nulls and guard intervals as shown in Tab. 2. It is worth noting that for reasons of standard compliance, only the data (192 subcarriers) are concerned with the PAPR reduction, the pilots and the guard intervals are not allowed to be modified when applying the proposed methods.

Tab. 2
Simulation parameters.

Parameters	Values
Channel Bandwidth	10 MHz
Modulation scheme	QPSK, 16-QAM, 64-QAM
FFT Size (NFFT)	256
Number of data subcarriers	192
Cyclic prefix or guard time	1/8
Pilots subcarriers	8
Null subcarriers	56

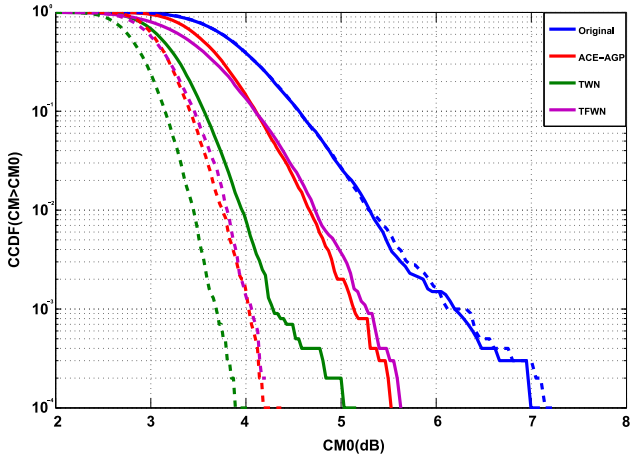

Fig. 4. CM reduction results using 16-QAM (solid) and QPSK (dashed).

5.1. Performance for QPSK and 16-QAM modulation modes

In Fig. 4, the curves shown represent the CM by using the Complementary Cumulative Distribution Function (CCDF). According to this figure, we note that the CM reduction for the proposed models compared to the original signal is about 28% against 22% for ACE-AGP for 16-QAM modulation, this proportion reaches 45% against 40% for ACE-AGP for QPSK modulation. Therefore, we assert that the proposals are well-suited for envelope fluctuation reduction in a WirelessMan–OFDM system. Furthermore, in comparison to the ACE-AGP algorithm in terms of CM criteria, the TFWN scheme gives similar performance, while the proposal TWN scheme reduces the CM with 0.3 dB and 0.5 dB respectively for QPSK and 16-QAM modulations. Besides, the loss in performance of the proposed TFWN scheme with respect to the TWN model is below 0.5 dB.

In order to show the effectiveness of our proposals, a BER performance in comparison with the original and ACE-AGP signal when using AWGN channel is performed. We deduce from Fig. 5 that the TFWN gives the best performance, in terms of BER, with regard to the other schemes. This can be explained by the fact that the proposed TFWN concentrates the energy even more than ACE-AGP. For low SNR, all schemes give similar performance with a

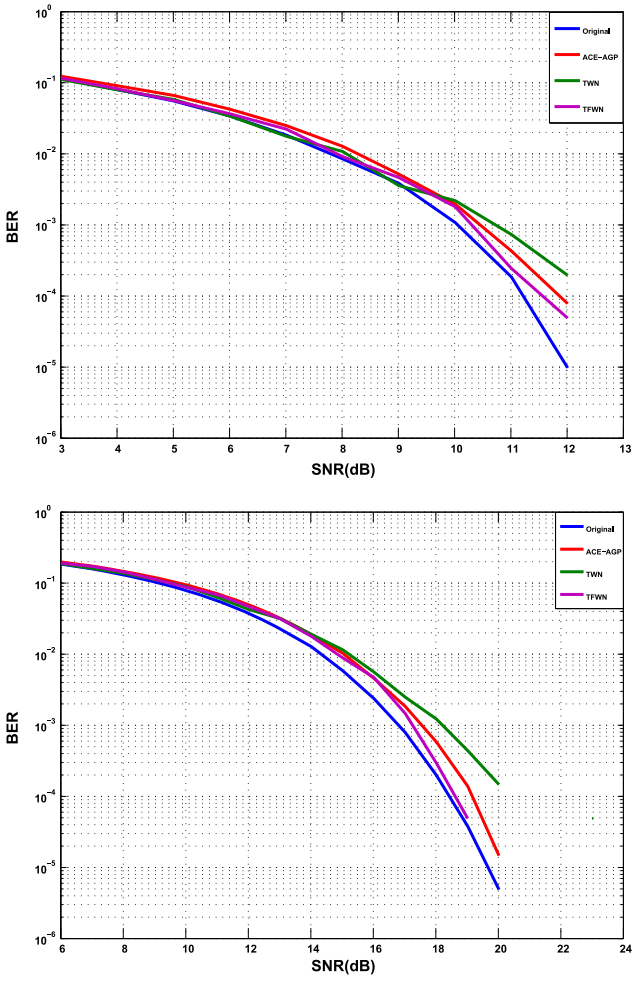

Fig. 5. BER comparison for different schemes for QPSK (above) and 16-QAM (below).

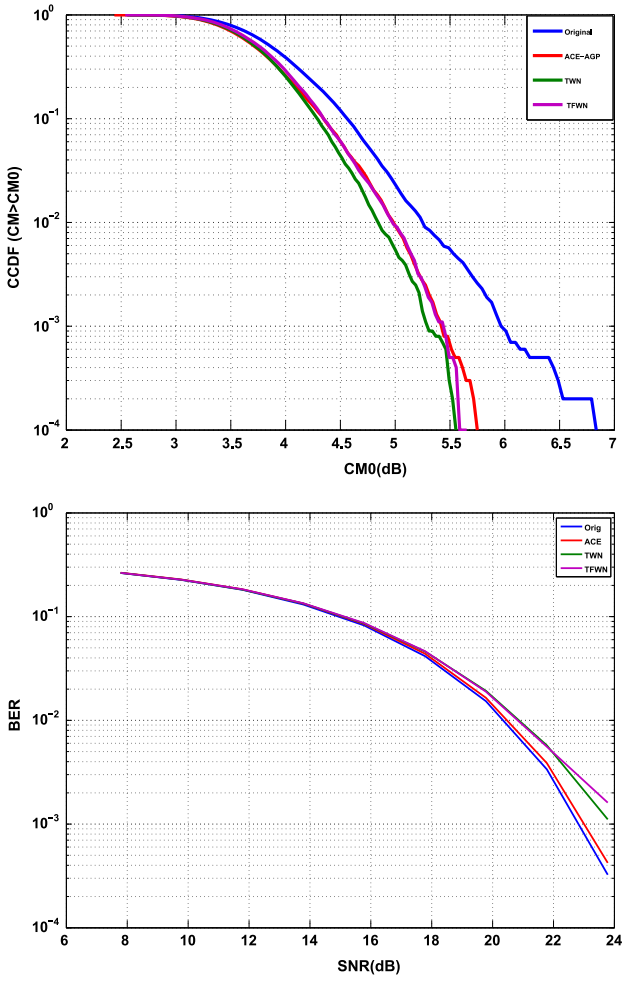

Fig. 6. Comparison of CM reduction results using 64-QAM (above) BER comparison for different schemes for 64-QAM (below).

slight advantage for our proposals. It is worth noting that Fig. 5 confirms the observation previously cited that the symbols placed into the not-allowable region degrade the performance of the TWN model for high SNR.

5.2. Performance for 64-QAM modulation mode

The IEEE 802.16d standard preconize for WirelessMan–OFDM physical layer, in addition to QPSK and 16-QAM, the 64-QAM as modulation modes. Fig. 6 presents the performance for high order modulation such as 64-QAM of our proposals in comparison with ACE-AGP in terms of CM reduction and BER vs SNR respectively.

It is seen that for 64-QAM the proposals perform better than the ACE-AGP in terms of the CM reduction criteria, the difference is about 0.2 dB. Thus, the CM reduction of our proposals reaches 1.2 dB against 1 dB for the ACE-AGP algorithm. For BER vs SNR the proposed models provide similar performance in comparison with the ACE-AGP algorithm. However, we must point out that the obtained performance of our proposals is achieved without the complexity and large required number of iterations of the ACE-AGP or other similar methods cited previously.

6. Conclusion

In this paper, we have used the wavelet networks systems in order to develop two models with the aim to reduce the PAPR in WirelessMan–OFDM systems. The simulation results show that the proposed models provide satisfactory results in terms of CM reduction criteria and BER vs SNR performance. Therefore, our proposals can be used as an alternative method to overcome the envelope fluctuations problem, even for high order modulation such as 64-QAM.

References

[1] J.G. Andrews, A. Ghosh, R. Muhamed, Fundamentals of WiMAX: Understanding Broadband Wireless Networking, Prentice Hall, Upper Saddle River, NJ, 2007.
[2] A. Ghosh, et al. Broadband Wireless Access with WiMAX/802.16: Current Performance Benchmarks and Future Potential. IEEE Commun. Mag. 43 (2005) 129–136.
[3] S. Srikanth, P.A. Murugesa Pandian, X. Fernando, Orthogonal frequency division multiple access in WiMAX and LTE: a comparison, IEEE Commun. Mag. 50 (9) (2012).
[4] S.H. Han, J.H. Lee, An overview of peak-to-average power ratio reduction techniques for multicarrier transmission, IEEE Wirel. Commun. 12 (2) (2005) 56–65.
[5] B.S. Krongold, D.L. Jones, PAR reduction in OFDM via active constellation extension, IEEE Trans. Broadcast. 49 (3) (2003) 258–268.
[6] H.-Y. Tseng, Y.-H. Chung, S.-M. Phoong, Y.-P. Lin, A reduced complexity PTS scheme for peak-to-average power ratio reduction in OFDM systems, in: Proceedings of EUSIPCO, 2008.
[7] S.-J. Heo, H.-S. Noh, J.-S. No, D.-J. Shin, A modified SLM scheme with low complexity for PAPR reduction of OFDM systems, IEEE Trans. Broadcast. 53 (4) (2007) 804–808.
[8] S. Khademi, et al., Peak-to-Average-Power-Ratio (PAPR) reduction in WiMAX and OFDM/A systems, EURASIP J. Adv. Signal Process. (2011), http://dx.doi.org/10.1186/1687-6180-2011-38.
[9] V.P.G. Jimnez, Y. Jabrane, A.G. Armada, B.A.E. Said, A.A. Ouahman, Reduction of

the envelope fluctuations of multi-carrier modulations using adaptive neural fuzzy inference systems, IEEE Trans. Commun. 59 (1) (2011) 19–25.
[10] Y. Jabrane, V.P.G. Jimnez, A.G. Armada, B.A.E. Said, A.A. Ouahman, Reduction of power envelope fluctuations in OFDM signals by using neural networks, IEEE Commun. Lett. 14 (2010) 99–601.
[11] S.A. Billings, H.-L. Wei, A new class of wavelet networks for nonlinear system identification, IEEE Trans. Neural Netw. 16 (4) (2005) 862–874.
[12] K. Antonios Alexandridis, D. Achilleas Zapranis, Wavelet neural networks: a practical guide, Neural Netw. 42 (2013) 1–27.
[13] TDoc R1-060023, Cubic Metric in 3GPP-LTE, 3GPP TSG RAN WG1, Technical Report, 2006.
[14] D.W. Marquardt, An algorithm for least-squares estimation of nonlinear parameters, J. Soc. Ind. Appl. Math. 11 (2) (1963) 431–441.
[15] Y. Oussar, G. Dreyfus, Initialization by selection for wavelet network training, Neurocomputing 34 (2000) 131–143.